HETEROCYCLES, Vol. 84, No. 2, 2012, pp. 719 - 735. ©2012 The Japan Institute of Heterocyclic Chemistry
Received, 22nd June, 2011, Accepted, 4th August, 2011, Published online, 17th August, 2011
DOI: 10.3987/COM-11-S(P)46

COMPUTATIONAL ASSESSMENT OF 1,3-DIPOLAR CYCLOADDITION OF NITRILE OXIDES WITH ETHENE AND [60]FULLERENE

Lydia Rhyman,[a] Sabina Jhaumeer-Laulloo,[a] Luis R. Domingo,[b] John A. Joule,[c] and Ponnadurai Ramasami[a]*

[a] Department of Chemistry, University of Mauritius, Réduit, Mauritius

[b] Departamento de Química Orgánica, Universidad de Valencia, Dr. Moliner 50, 46100 Burjassot, Valencia, Spain

[c] The School of Chemistry, The University of Manchester, Manchester M13 9PL, UK

* Corresponding author email: ramchemi@intnet.mu

Abstract – The 1,3-dipolar cycloaddition (1,3-DC) reactions of ethene and [60]fullerene with nitrile oxides, **RCNO**, have been studied in the gas phase, using DFT method at the B3LYP/6-31G(d) level. Energetics, thermodynamic and kinetic parameters have been determined at room temperature so as to investigate the effect of electron-withdrawing and electron-releasing substituents attached to the nitrile oxides on the 1,3-DCs. These parameters have been interpreted in terms of group electronegativity and reactivity indices. An atypical behavior has been observed for the 1,3-DC involving **FCNO** as it has some pseudodiradical character.

INTRODUCTION

Since the discovery of buckminsterfullerene, C_{60}, more than two decades ago by Kroto *et al.*[1] and its synthesis by Krätshmet *et al.*,[2] fullerene chemistry has become one of the most vigorously developing fields in organic chemistry. [60]Fullerene-based derivatives have attracted particular attention of researchers from both experimental and theoretical point of views. Due to the great diversity of functionalizations of the C_{60} spheroid,[3] these [60]fullerene-based materials have found applications ranging from non-linear optics to extreme hardness, molecular electronics and superconductivity.[4] For instance, functionalized C_{60} compounds offer wide opportunities for the creation of new nanocarbons with potential application in biological,[5] material science[6] and medicinal chemistry.[7] C_{60} has also been functionalized by organometallic reagents.[8] Very recently, Podolski *et al.*[9] reported the development of

drugs based on C_{60} which are becoming increasingly important as they act on the key molecular mechanisms at the early stage of Alzheimer's disease.

C_{60} is an electron deficient polyolefin and it is known to undergo various types of reaction such as reduction, halogenation, radical addition, nucleophilic addition, mono- and polycyclic addition.[10] However, in the 1990s, several studies revealed that the most employed and straightforward procedures for functionalization of C_{60} are cycloaddition reactions.[11] Of particular interest is the 1,3-dipolar cycloaddition (1,3-DC) which plays an important role in the preparation of functionalized C_{60} compounds.[12] Suzuki *et al.*[13] showed that C_{60} is a reactive dipolarophile by carrying out a systematic experimental investigation of its reaction with substituted diazomethanes. Since then, various 1,3-dipoles, such as azomethine ylides, diazo compounds, azides, nitrile oxides, nitrile ylides, nitrile imines, pyrazolinium ylides and carbonyl ylides have been reported to react with C_{60}.[3,11,14]

1,3-DCs have been used to synthesize [60]fullerene-fused heterocycles and these reactions have been the subject of several experimental and theoretical studies.[15] C_{60} reacts with various nitrile oxides providing a series of fulleroisoxazolines with diverse substitutents. These fulleroisoxazolines show appealing chemical, electrochemical and photochemical properties.[16] During the last years, several experimental reports on the 1,3-DC of substituted nitrile oxides to C_{60} have appeared.[17] The parent fullereneisoxazole (**R** = **H**) was synthesized by heating a mixture of C_{60} and chlorooximidoacetic.[17e] NMR spectroscopy showed that a single isomer was obtained resulting from addition across a [6,6] ring fusion.[17e] Furthermore, nitrile oxides bearing different substitutents such as alkyl, aryl and other bulky substituents were also added to C_{60} and the structures of the cycloadducts (CAs) were established by X-ray diffraction analysis.[17c-e] The reactions of some simple nitrile oxides with C_{60} have also been modeled and studied theoretically by Kavitha and Venuvanalingam[18] at the B3LYP/6-31G(d,p)//AM1 level. Although there was controversy over the concerted or stepwise nature of these mechanisms, they found that the closed [6,6] adducts are the most stable and a concerted mechanism is followed; the stepwise mechanism is higher in energy than the corresponding concerted one.

In order to have a better insight into the 1,3-DC of unsubstituted (**HCNO**) and substituted nitrile oxides (**RCNO**), with electron-releasing (ER) substitutents (**R** = **Me** and **Et**) and electron-withdrawing (EW) substituents (**R** = **F**, **Cl**, **Br**, **NC**, **CN** and **NO_2**), with C_{60} (Scheme 1), we report a systematic DFT study, by means of B3LYP/6-31G(d) computations. We have also studied, for comparison, the 1,3-DC of these nitrile oxides to ethene. Energetics, thermodynamic and kinetic parameters of these reactions are investigated. In addition, the features of the reaction mechanism such as synchronicity, nature of

transition state structure (TS), charge transfer (CT), analysis of the reactivity indices and the rate constants of these 1,3-DCs are also taken into consideration. The results obtained are critically analyzed and discussed.

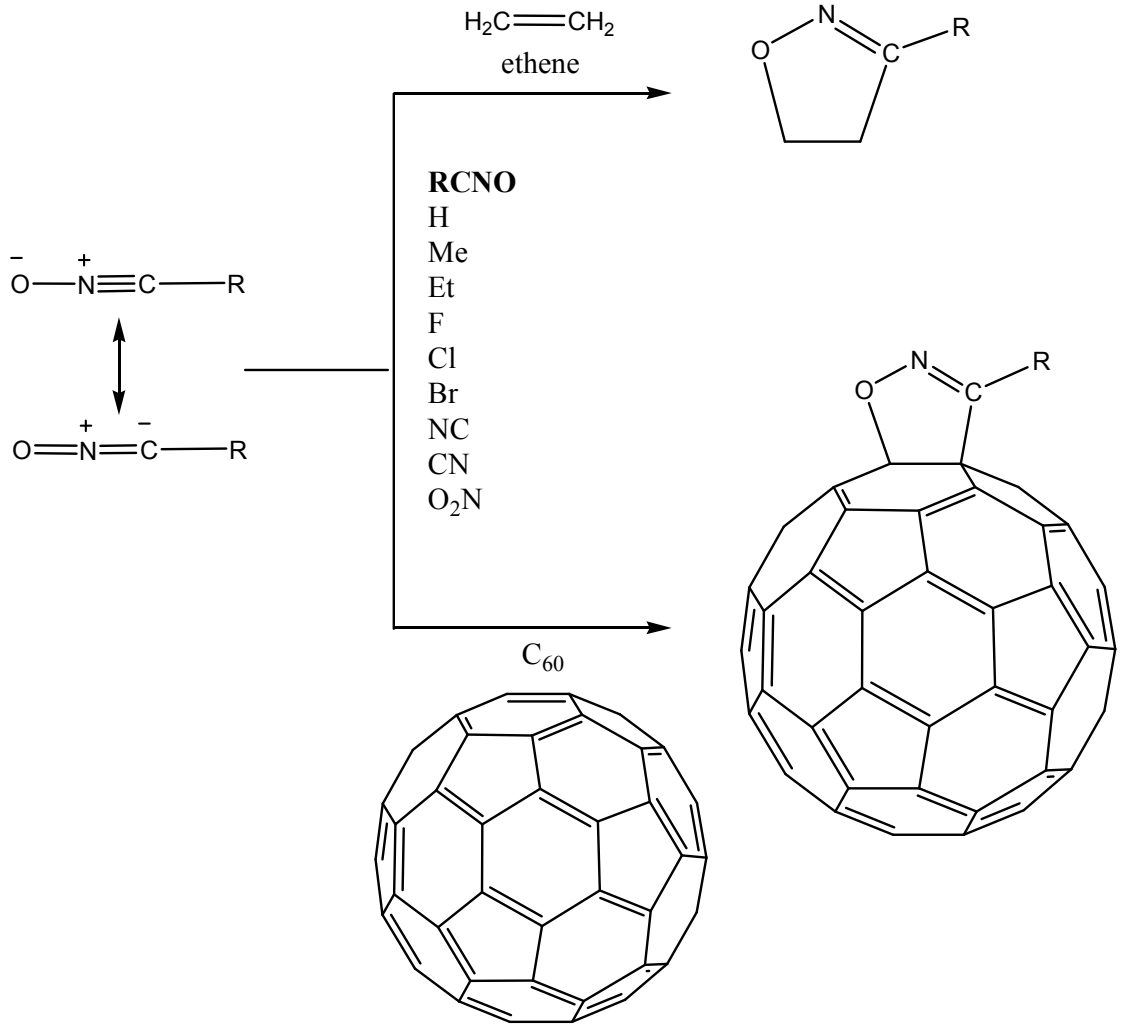

Scheme 1. Model reactions for the 1,3-DC of RCNO with ethene and C_{60}

RESULTS AND DISCUSSION

ENERGETICS

Table 1 lists the relative gas phase energies for the 1,3-DC of nitrile oxides with ethene and C_{60}. 1,3-DC can occur at [6,6] or [5,6] bond of C_{60} and can form closed and open CAs. Therefore, the reaction can proceed through four types of additions; closed [6,6], closed [5,6], open [6,6] and open [5,6]. Also, each of these modes of addition can follow either concerted or stepwise pathways. However, only the closed [6,6] pathway is taken into consideration as it leads to the most stable CA as supported by various studies.[18]

Table 1. Relative energies[a] (kJ mol^{-1}) including ZPE computed at 298.15 K and 1 atm for the gas phase reactions of **RCNO** with ethene and C_{60}

R	**H**	**Me**	**Et**	**F**	**Cl**	**Br**	**NC**	**CN**	**NO_2**
					RCNO + $H_2C=CH_2$				
TS	55.7	58.2	56.9	6.5	30.5	36.6	49.7	31.3	16.2
CA	-166.7	-160.4	-159.6	-270.7	-214.7	-201.1	-167.4	-205.3	-239.9
					RCNO + C_{60}				
TS	51.6	49.5	48.1	5.8	29.7	32.6	53.8	32.9	17.5
CA	-104.9	-101.3	-100.7	-207.9	-148.4	-139.6	-98.2	-138.0	-166.1

[a] *Relative to **RCNO** + ethene or **RCNO** + C_{60}.*

An analysis of Table 1 allows some noteworthy features to be observed. For the reaction of **RCNO** + ethene, the activation energy increases in the following order **R** = **F** < **NO_2** < **Cl** < **CN** < **Br** < **NC** < **H** < **Et** < **Me** and **R** = **F** < **NO_2** < **Cl** < **CN** ≈ **Br** < **Et** < **Me** < **H** < **NC** for the reaction of **RCNO** + C_{60}. Additionally, the reaction energy for the formation of the CAs increases in the order **R** = **Et** < **Me** < **H** < **NC** < **Br** < **CN** < **Cl** < **NO_2** < **F** for the reaction of **RCNO** + ethene and **R** = **NC < Et < Me < H < CN < Br < Cl < NO_2 < F** for the reaction of **RCNO** + C_{60}. The activation energies are higher for the reaction with ethene than with C_{60}, except for **R** = **NC**, **CN** and **NO_2**. Similarly, the 1,3-DCs of substituted nitrile oxides with ethene are more exothermic than with C_{60}. In general, the presence of ER groups on the 1,3-dipole increases the activation energy compared to the EW groups. On comparing the unsubstituted nitrile oxide (**R** = **H**) with those attached to ER groups, it can be found that they have comparable activation energy. In addition, for the reaction of C_{60}, the activation energy decreases slightly from **R** = **Me** to **Et** due to an increase in nucleophilicity. However, based on the relative energies with respect to their reactants, the CAs bearing an alkyl substituent are slightly less stable than one with unsubstituted nitrile oxide (**R** = **H**). Conversely, the presence of an EW substituent on the nitrile oxide decreases the activation energy relative to the parent nitrile oxide. Moreover, the activation energy drastically decreases when **R** = **F**. The same trend is observed with the relative energy for both ethene and C_{60}.

We have attempted to correlate the predicted activation energy with electronegativity of the substituent on the nitrile oxides based on the Pauling electronegativity scale and 'super-atom' approximation.[19] Figure 1 displays the group electronegativity of the substituents while Figure 2 illustrates the activation energy against the nitrile oxides. It can be observed that the predicted activation energy is inversely proportional to the group electronegativity. Moreover, **FCNO** is the most electronegative dipole followed by **O_2NCNO** and as a result, a similar trend is noted for the activation energy, whereby the activation energy for the 1,3-DC of **FCNO** with both ethene and C_{60} is lowest followed by the 1,3-DC of **O_2NCNO**. On comparing the cyano and isocyano substituents, it can be found that the cyano substituent has lower activation energy compared to the isocyano substituent and this can be explained by the higher electronegativity of the isocyano group[20] compared to the cyano group, as shown in Figure 1. The same

variation is observed on considering the relative energy of these two substituents.

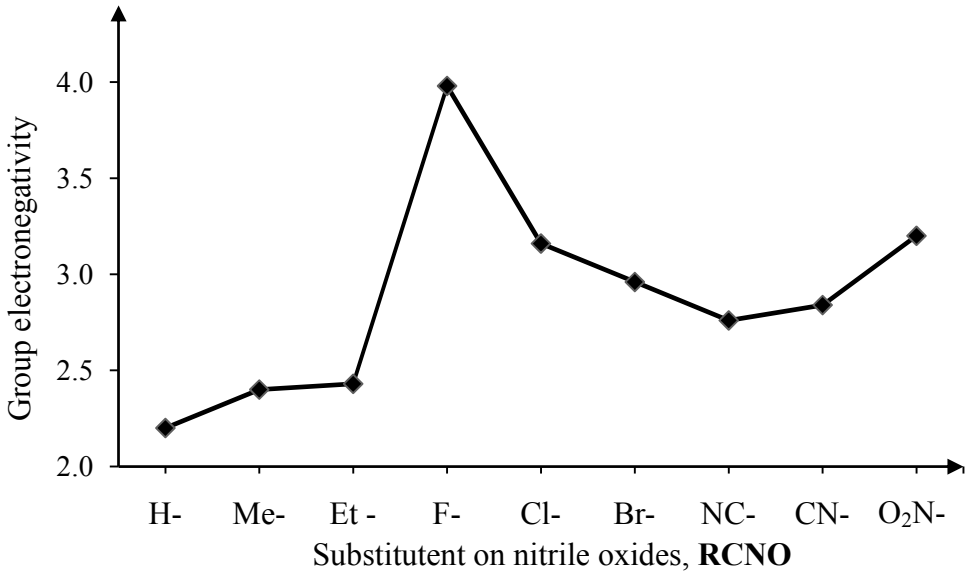

Figure 1. Group electronegativity of the substituent on the nitrile oxides

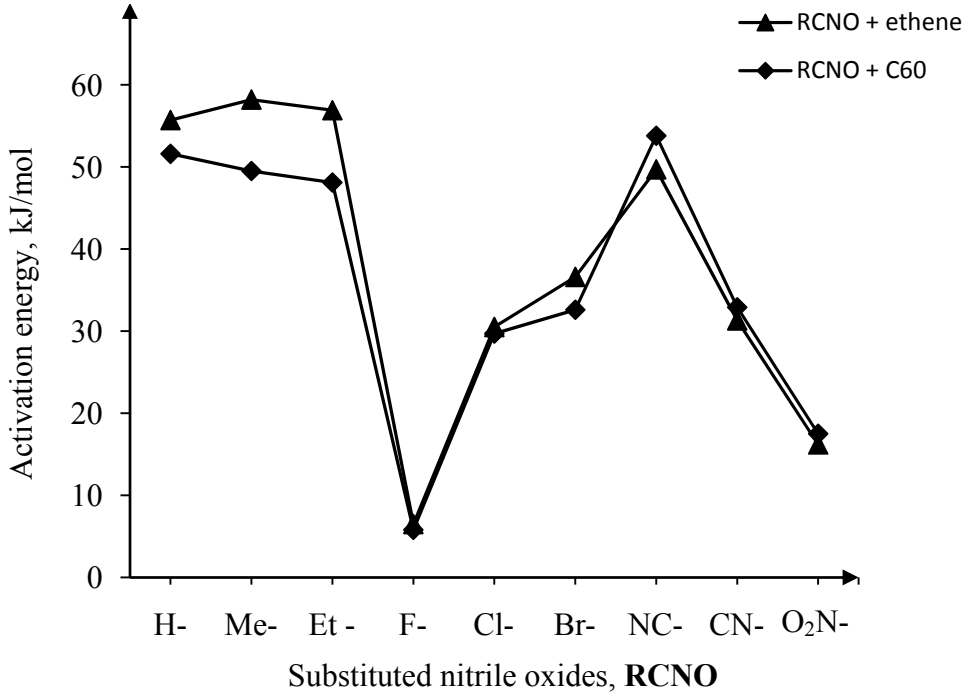

Figure 2. Activation energy for the 1,3-DC of nitrile oxides with ethene and C_{60}

The thermodynamic parameters namely activation enthalpies and activation Gibbs free energies as well as the reaction enthalpies and reaction Gibbs free energies computed at 298.15 K and 1 atm are gathered in Table 2. The activation enthalpy increases in the following order **R** = **F** < **NO_2** < **Cl** < **CN** < **Br** < **NC** < **H** < **Et** < **Me** for **RCNO** + ethene and **R** = **F** < **NO_2** < **Cl** < **CN** < **Br** < **Et** < **Me** < **H** < **NC** for **RCNO** + C_{60} and this is in conformity with the activation energies. In addition, the reaction enthalpy follows the

same trend as the relative energy calculated in Table 1, thereby indicating that these 1,3-DCs are exothermic processes.

Table 2. Relative enthalpies[a] (ΔH, in kJ mol^{-1}), free energies (ΔG, in kJ mol^{-1}) and entropies (ΔS, in J mol^{-1} K^{-1}) computed at 298.15 K and 1 atm for the TSs and CAs involved in the gas phase reactions of **RCNO** with C_{60}

R	H	Me	Et	F	Cl	Br	NC	CN	NO_2
RCNO + $H_2C=CH_2$									
				ΔH					
TS	49.7	54.2	53.2	3.8	26.8	33.2	46.1	27.4	13.8
CA	-175.6	-167.8	-166.2	-278.0	-221.9	-207.9	-173.7	-212.5	-246.4
				ΔG					
TS	96.5	99.8	102.2	48.0	73.1	64.0	81.4	59.3	61.9
CA	-124.1	-114.4	-110.0	-223.2	-167.8	-169.6	-135.1	-174.3	-188.3
				ΔS					
TS	-156.8	-153.0	-164.4	-148.1	-155.2	-103.3	-118.5	-107.0	-161.3
CA	-172.6	-179.0	-188.7	-183.7	-181.6	-128.4	-129.4	-128.3	-195.5
RCNO + C_{60}									
				ΔH					
TS	49.0	49.1	48.1	6.2	29.6	32.8	53.9	32.5	18.0
CA	-110.8	-105.2	-103.4	-211.5	151.7	-142.3	-101.0	-141.5	-169.1
				ΔG					
TS	98.0	98.0	100.7	52.7	79.5	67.5	92.5	67.6	72.7
CA	-52.2	-44.9	-40.3	-150.5	-90.7	-96.9	-52.6	-95.8	-101.5
				ΔS					
TS	-125.0	-164.0	-176.3	-155.9	-167.4	-116.2	-129.4	-117.6	-183.4
CA	-157.3	-202.3	-211.8	-204.4	-204.7	-152.3	-162.6	-153.4	-227.0

[a] *Relative to **RCNO** + ethene or **RCNO** + C_{60}.*

GEOMETRICAL PARAMETERS OF TRANSITION STATES

The geometries of the TSs for each 1,3-DC are presented in Figures 3-4. An analysis of the lengths of the two forming bonds at the TSs indicates that these reactions are asynchronous concerted processes. The length of the C–O forming bond is longer than the C–C bond, suggesting that the formation of C–C bond is more advanced than the C–O bond. The values of the lengths of the two forming bonds at the TSs are in the range of 2.351 – 2.644 Å and 2.228 – 2.543 Å for the C–O and C–C forming bonds, respectively, for reaction with ethene and in the range of 2.365 – 2.761 Å and 2.118 – 2.401 Å for the C–O and C–C forming bonds, respectively, for the reaction with C_{60}. The degree of asynchronicity of the 1,3-DCs can be determined by considering the difference between the lengths of the two forming bonds such that Δd = [d(C–O) – d(C–C)].[21] Table 3 reports the degree of asynchronicity, Δd, of the TSs. Overall, the TSs display varying degrees of asynchronicity depending on the substituent present on the nitrile oxide. Greater asynchronicity is observed for the 1,3-DC of nitrile oxide with C_{60} than with ethene, which is due to the polarity of both the 1,3-dipoles and dipolarophiles. Moreover, a comparison of the Δd for these

1,3-DCs indicates that Δd is largest when **R** = **NO_2** and hence, it is the most asynchronous. On the other hand, the more synchronous TSs arise from the reaction of **MeCNO** and **EtCNO** with C_{60}. It can be concluded that presence of an EW group on the nitrile oxide forms CA through more asynchronous TSs (**R** = **NO_2**), while the presence of an ER group on the nitrile oxide affords more synchronous TSs (**R** = **Et**).

Table 3. Δd at the TSs arising from the 1,3-DC of **RCNO** with ethene and C_{60}

R	**H**	**Me**	**Et**	**F**	**Cl**	**Br**	**NC**	**CN**	**NO_2**
				RCNO + H_2C=CH_2					
Δd	0.18	0.12	0.10	0.04	0.11	0.11	0.13	0.07	0.28
				RCNO + C_{60}					
Δd	0.43	0.23	0.25	0.34	0.28	0.33	0.34	0.31	0.49

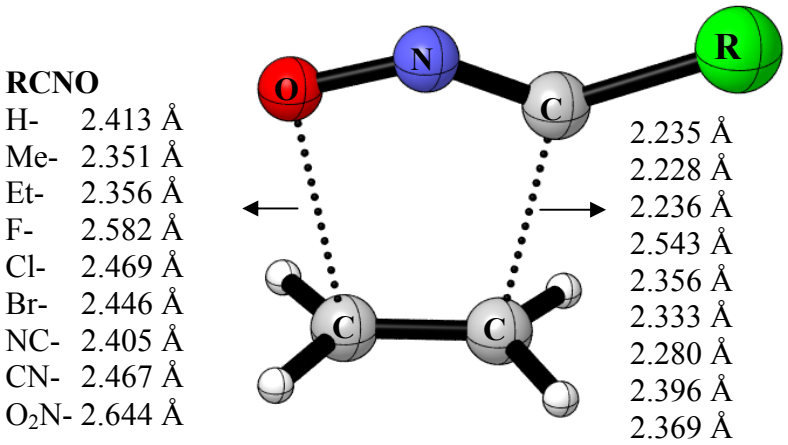

Figure 3. Optimized geometries of the TSs involved in the 1,3-DCs between nitrile oxides with ethene

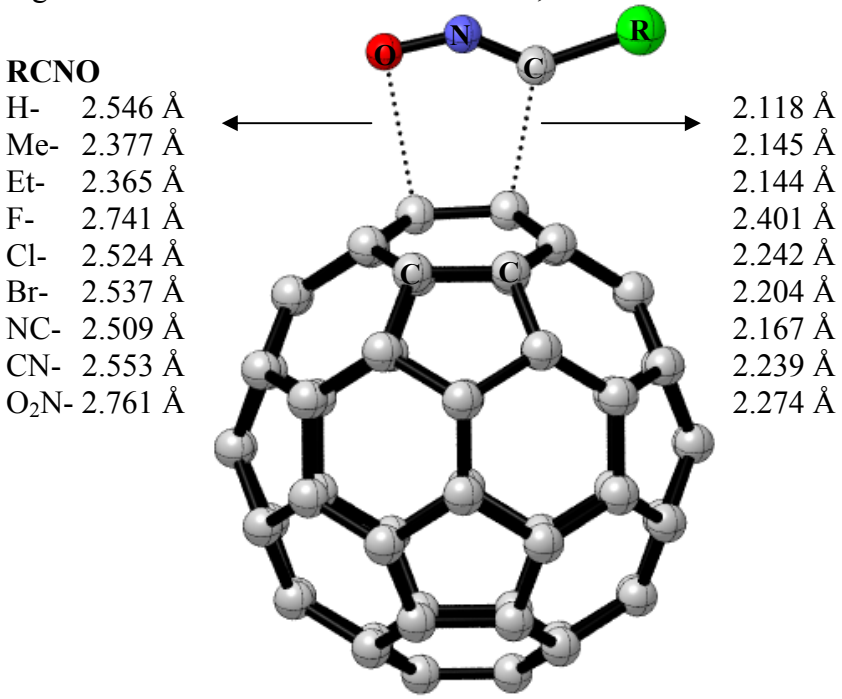

Figure 4. Optimized geometries of the TSs involved in the 1,3-DCs between nitrile oxides with C_{60}

BOND ORDER AND CHARGE TRANSFER

The Wiberg bond indices[22] have been computed to follow the nature of the cycloaddition process using NBO analysis. The bond order (BO) analysis of the TS arising from the 1,3-DCs of ethene and C_{60} with substituted nitrile oxides shows asynchronicity of the bond formation processes. The BO values of the two forming bonds at the TSs for the 1,3-DCs are reported in Table 4.

The BO values for the C–C forming bond at the TSs are larger than those for the C–O bond. For the 1,3-DCs with C_{60}, while the C–C BO values increase relative to the reactions with ethene, the C–O BO values decrease, indicating that the TSs are more advanced and more asynchronous. Thus, for the reaction with ethene the BO values range from 0.15 to 0.30 and 0.12 to 0.22 for the C–C and C–O forming bonds, whereas for the reaction with C_{60} they range from 0.17 to 0.33 and 0.08 to 0.18 for the C–C and C–O forming bonds, respectively. It is noteworthy that the presence of an EW group on nitrile oxide results in a low BO value for both the C–O and C–C bond formation processes.

Table 4. Wiberg bond orders of the TSs involved during the 1,3-DCs of nitrile oxides with ethene and C_{60}

	RCNO + H_2C=CH_2		**RCNO + C_{60}**	
	C–O	C–C	C–O	C–C
HCNO	0.21	0.30	0.14	0.33
MeCNO	0.22	0.30	0.18	0.32
EtCNO	0.22	0.29	0.18	0.32
FCNO	0.12	0.15	0.08	0.17
ClCNO	0.17	0.22	0.13	0.25
BrCNO	0.19	0.24	0.13	0.27
NCCNO	0.20	0.26	0.14	0.30
CNCNO	0.17	0.22	0.12	0.25
O_2NCNO	0.13	0.19	0.08	0.24

The electronic nature of these 1,3-DCs is evaluated by analyzing the CT at the TSs. The natural atomic charges are shared between the nitrile oxides and the dipolarophiles, ethene and C_{60}, and these data are shown in Table 5. For the reactions with ethene, the natural population analysis gives a negligible CT, which takes place from ethene to the nitrile oxides. These low CTs point out non polar processes with some pseudodiradical character.[23] It is to be noted that CT increases slightly with the EW character of the substituent. The 1,3-DCs with C_{60}, also present very low CT; however, at these cycloadditions, the flux of the electron density depends on the nature of the substituent present on nitrile oxide. Thus, while for the ER **Me** and **Et** groups the CT fluxes towards C_{60}, for the EW **CN** and **NO_2** groups the CT fluxes towards the nitrile oxide.

Table 5. Charge transfer (CT, in e), dipole moment (DM, in Debye) and imaginary frequency (IF, in cm^{-1}) of TSs

R	H	Me	Et	F	Cl	Br	NC	CN	NO_2
					RCNO + H_2C=CH_2				
CT	-0.02	-0.01	-0.01	-0.02	-0.04	-0.05	-0.08	-0.05	-0.07
DM	2.462	3.250	3.310	1.465	1.788	2.009	2.542	1.588	2.322
IF	-406.3	-407.4	-389.2	-170.8	-304.9	-319.5	-367.8	-301.6	-241.7
					RCNO + C_{60}				
CT	0.05	0.08	0.08	0.01	0.01	0.02	-0.05	-0.02	-0.07
DM	2.127	3.222	3.489	1.364	1.584	1.960	2.997	1.797	3.121
IF	-400.3	-388.6	-361.3	-137.4	-301.9	-326.2	-371.6	-301.7	-229.0

All TSs have only one imaginary vibrational frequency, corresponding to the atomic motion along the direction of the newly forming bonds. The values for the imaginary frequencies, in the range 409.1*i* – 170.8*i* cm^{-1} and 400.3*i* –137.4*i* cm^{-1} for the 1,3-DCs with ethene and C_{60}, respectively, are reported in Table 5. The imaginary frequency values for the ER substituted nitrile oxides are slightly lower than for the EW substituted ones. These low values indicate that these processes are associated with heavy atom motions and are also related to the earlier TSs. It is noteworthy that the TSs bearing fluorine have the lowest imaginary frequency.

REACTIVITY INDICES

Recent studies[24] carried out on cycloaddition reactions have shown that the reactivity indices defined within the conceptual DFT are powerful tools for establishing the polar character of such reactions. Table 6 shows the static global properties, namely electronic chemical potential (μ), chemical hardness (η), global electrophilicity (ω), and global nucleophilicity (N), of C_{60}, ethene and the substituted nitrones.

Table 6. Electronic chemical potential (μ), chemical hardness (η), global electrophilicity (ω), and global nucleophilicity (N), in eV, of C_{60}, ethene and substituted nitrile oxides

	μ	η	ω	N
C_{60}	−4.61	2.76	3.84	3.13
O_2NCNO	−5.97	4.70	3.79	0.80
FCNO	−4.92	5.05	2.40	1.67
NCCNO	−5.26	6.09	2.27	0.82
CNCNO	−4.84	5.96	1.96	1.30
ClCNO	−4.26	5.98	1.52	1.87
BrCNO	−4.15	5.83	1.48	2.06
Ethene	−3.37	7.76	0.73	1.87
HCNO	−3.40	7.94	0.73	1.75
EtCNO	−2.91	7.51	0.56	2.46
MeCNO	−2.90	7.66	0.55	2.39

The electronic chemical potential of C_{60} is μ = −4.61eV. On the other hand, for the nitrile oxides the electronic chemical potential ranges from μ = −2.90 eV for **MeCNO** to μ = −5.97 eV for **O_2NCNO**. Therefore, it is expected that in a polar process the flux of the CT depends on the nature of the substituent present on nitrile oxide. The electrophilicity of C_{60}, ω = 3.84 eV, allows for the classification of this species as a strong electrophile within the electrophilicity scale.[24a] On the other hand, a high nucleophilicity value, N = 3.13 eV, is predicted for C_{60} and thus, it is classified as a strong nucleophile within the nucleophilicity scale.[25] Ethene has low electrophilicity and nucleophilicity values, ω = 0.73 eV and N = 1.87 eV. Therefore, it is expected that ethene does not participate in polar processes, in clear agreement with the low CT found in these 1,3-DCs.[23]

The electrophilicity of the substituted nitrile oxides ranges from ω = 3.79 eV for **O_2NCNO** to ω = 0.55 eV for **MeCNO**. A good correlation can be found between the EW or ER character of the substituent and the electrophilicity of the corresponding nitrile oxide. Thus, while **O_2NCNO** is the most electrophilic, **MeCNO** is the poorest electrophilic nitrile oxide. The nucleophilicity of the nitrile oxides ranges from 2.39 to 0.80 eV. In general the increase of the electrophilic character of the nitrile oxides can be related with the decrease of the nucleophilic one.

Analysis of the CT at the TSs of the 1,3-DCs with C_{60}, indicates that they take place with a low polar character. In spite of this behavior, if the faster reaction, **FCNO**, and the slowest one, **NCCNO**, are discarded of the series, a reasonable correlation is found between the electrophilicity of nitrile oxides **RCNO** and the activation energy of the 1,3-DC with R^2 = 0.87 as illustrated in Figure 5. In addition, considering the electronic chemical potential of C_{60}, we can explain the change of the flux of the CT on the 1,3-DC reactions included in Figure 6 (see Table 5); **O_2NCNO** (−5.97 eV) < **NCCNO** (−5.26 eV) < C_{60} (−4.61 eV) < **ClCNO** (−4.26 eV) < **BrCNO** (−4.15 eV) < **HCNO** (−3.40 eV) < **EtCNO** (−2.91 eV) < **MeCNO** (−2.90). Thus, while for the 1,3-DCs with; **O_2NCNO** and **NCCNO** the charge fluxes from C_{60}, to these nitrile oxides, for the rest the charge fluxes towards C_{60}.

At this stage, it is interesting to comment on the 1,3-DCs with **FCNO**. The cycloadditions of this nitrile oxide with ethene and C_{60} are the fastest reactions, in spite of being less electrophilic than **O_2NCNO**. On the other hand, these reactions show the lowest CT, pointing to non polar processes. These behaviors suggest that the 1,3-DCs of **FCNO** can take place through earlier TSs with some pseudodiradical character,[26] which could be favored by the presence of the fluorine atom.

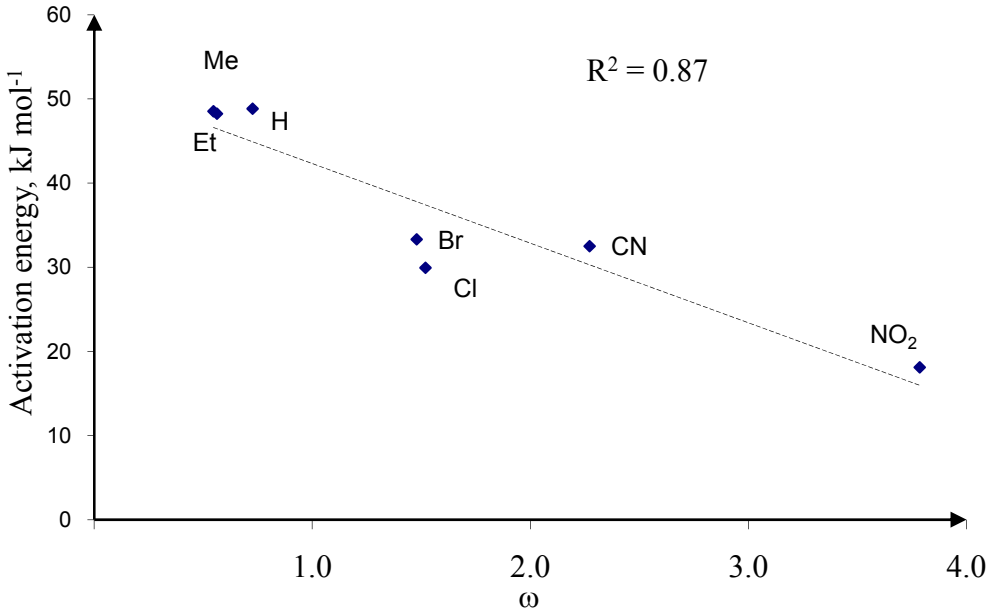

Figure 5. Plot of the activation energies (ΔE, in kcal/mol) associated with the 1,3-DCs of some substituted nitrile oxides with C_{60} *versus* the electrophilicity ω of the nitrile oxides

Although C_{60} has larger electrophilicity and nucleophilicity values than ethene (See Table 6), the comparable relative energies and the low CT for 1,3-DCs of these dipolarophiles with the **RCNO** series indicate that, like ethene,[23] the 1,3-DCs of C_{60} have non polar character. Despite of its pseudodiradical character, C_{60} appears to have some response to the electrophilic/nucleophilic behavior of **RCNOs** as shown in Figure 5.

RATE CONSTANTS

The rate constants for the second order elementary step, k_1 for the 1,3-DCs of the nitrile oxides with ethene and C_{60} are reported in Table 7. Our calculations show that $k_2 >> k_{-1}$ and thus, from equation (2), the effective rate constant k_{ef} is same as k_1. On comparing the 1,3-DC with ethene and C_{60} with nitrile oxides it is found that the larger rate constants, k_1, are associated with ethene. The rate constant increases in the order **Et** < **Me** < **H** < **NC** < **Cl** < **Br** < **NO_2** < **CN** < **F** for the reaction between **RCNO** with ethene and **Et** < **H** < **Me** < **NC** < **Cl** < **NO_2** < **CN** < **Br** < **F** for the reaction between **RCNO** with C_{60}. Thus, the reaction with **FCNO** is fastest compared to reaction with the other nitrile oxides. In general, the variations in the rate constants can be rationalized in terms of activation energies. It is important to note that there is a good agreement with the values of the k_1 calculated from equations (3) and (6).

Table 7. Rate constants, k_1, of the 1,3-DCs of nitrile oxides with ethene and C_{60}

RCNO	RCNO + $H_2C=CH_2$		RCNO + C_{60}	
	k_1^a	k_1^b	k_1^a	k_1^b
H	1.90	2.20	1.02	1.18
Me	4.95×10^{-1}	5.74×10^{-1}	1.04	1.19
Et	1.86×10^{-1}	2.12×10^{-1}	3.45×10^{-1}	3.88×10^{-1}
F	$6.01 \times 10^{+8}$	$6.17 \times 10^{+8}$	$8.82 \times 10^{+7}$	$9.75 \times 10^{+7}$
Cl	$2.39 \times 10^{+4}$	$2.60 \times 10^{+4}$	$1.82 \times 10^{+3}$	$1.98 \times 10^{+3}$
Br	$9.38 \times 10^{+5}$	$1.03 \times 10^{+6}$	$2.28 \times 10^{+5}$	$2.51 \times 10^{+5}$
NC	$8.34 \times 10^{+2}$	$9.42 \times 10^{+2}$	9.44	10.68
CN	$6.26 \times 10^{+6}$	$6.79 \times 10^{+6}$	$2.22 \times 10^{+5}$	$2.41 \times 10^{+5}$
NO_2	$2.19 \times 10^{+6}$	$2.31 \times 10^{+6}$	$2.77 \times 10^{+4}$	$2.91 \times 10^{+4}$

[a] *k_1 calculated from equation (3)*
[b] *k_1 calculated from equation (6)*

COMPUTATIONAL METHOD

Gas phase full geometries optimizations have been carried out with the Gaussian 03 suite of programs,[27] at the Becke's[28] (B3) and the correlation functional by Lee-Yang-Parr's[29] (LYP) density functional with the 6-31G(d) basis set.[30] Harmonic vibrational analysis was performed to verify each minimum on the potential energy surface. Every stationary point identified was characterized by the number of negative eigenvalues of their Hessian matrix; 0 for minima and 1 for any true TS. The imaginary frequencies also exhibit the expected motion and this was assigned by means of visual inspection and animation using CYLVIEW program.[31] The reported electronic energies include zero-point energies (ZPE) corrections. Further, the intrinsic reaction coordinate[32] (IRC) path was traced, at the same level of theory, to ensure that the TSs led to the expected reactants and products. Natural bond orbital (NBO) analysis was performed on the electronic structures of the critical points according to Weinhold and coworkers[33] as implemented in Gaussian 03.

The global electrophilicity index, ω, is given by the following simple expression,[34] $\omega = (\mu^2/2\eta)$, in terms of the electronic chemical potential μ and the chemical hardness η. Both quantities may be approached in terms of the one electron energies of the frontier molecular orbital HOMO and LUMO, ε_H and ε_L, as $\mu \approx (\varepsilon_H + \varepsilon_L)/2$ and $\eta \approx (\varepsilon_L - \varepsilon_H)$, respectively.[35] Recently, we have introduced an empirical (relative) nucleophilicity index, N based on the HOMO energies obtained within the Kohn-Sham scheme,[36] and defined as $N = \varepsilon_{H(Nu)} - \varepsilon_{H(TCE)}$. Tetracyanoethylene (TCE) is chosen as reference as it presents the lowest HOMO energy in a large series of molecules already investigated in the context of polar cycloadditions. This choice allowed us conveniently to handle a nucleophilicity scale of positive values.[37]

The rate constant, calculated at 298.15 K, is predicted according to the following equation (1):

$$\mathbf{1} + \mathbf{2} \underset{k_{-1}}{\overset{k_1}{\rightleftharpoons}} \mathbf{TS} \xrightarrow{k_2} \mathbf{CA} \qquad (1)$$

The effective rate constant corresponding to the formation of CAs can, thus, be calculated as:

$$k_{ef} = \frac{k_1 k_2}{k_{-1} + k_2} \qquad (2)$$

The rate constant of each step is calculated based on the conventional transition state theory[38] (TST) equations:

$$k_1 = \kappa \frac{k_B T}{h} \frac{RT}{p} exp \frac{\Delta S^\circ}{R} exp\left(-\frac{\Delta H^\circ}{RT}\right) \qquad (3)$$

$$k_{-1} = \kappa \frac{k_B T}{h} exp\left(-\frac{\Delta S^\circ}{R}\right) exp \frac{\Delta H^\circ}{RT} \qquad (4)$$

$$k_2 = \kappa \frac{k_B T}{h} exp\left(\frac{\Delta S^{\neq}}{R}\right) exp\left(-\frac{\Delta H^{\neq}}{RT}\right) \qquad (5)$$

where k_B is Boltzmann's constant; h is Planck's constant, T is the temperature; R is the ideal gas constant; κ is the transmission coefficient and is taken to be 1; ΔH° is the relative enthalpy, $\Delta H^{\neq}$ is the activation enthalpy while ΔS° and $\Delta S^{\neq}$ are the relative and activation entropies, respectively.

In addition, k_1, has also been calculated with the Wigner tunneling coefficient[38c,39] according to the standard Eyring TST as:

$$k_1 = \Gamma \frac{k_B T}{h} \frac{Q_{TS} N_A}{Q_1 Q_2} exp\left(-\frac{\Delta E_a}{RT}\right) \qquad (6)$$

where N_A is the Avogadro's number; Q_{TS}, Q_1 and Q_2 are the total partition functions of TS, **1** and **2**, respectively and ΔE_a is the activation energy for the cycloaddition. The values of the rate constants are calculated at standard conditions (T = 298.15 K and p = 101325 Pa).

CONCLUSIONS

The 1,3-DCs of nitrile oxides with ethene and C_{60}, yielding fulleroisoxazolines, have been studied using DFT computations at the B3LYP/6-31G(d) level. The influence of EW and ER substituents on the reactivity has been determined in the closed [6,6] pathway in the gas phase. The activation energies for the reaction of **RCNO** + ethene follow the order **R** = **F** < **NO_2** < **Cl** < **CN** < **Br** < **NC** < **H** < **Et** < **Me** which is in agreement with the reaction **RCNO** + C_{60}, **R** = **F** < **NO_2** < **Cl** < **CN** < **Br** < **Et** < **Me** < **H** < **NC** with only **NC** misplaced. These predicted activation energies are inversely proportional to the group electronegativity of the substituent. The calculated thermodynamic parameters are also in line with the activation energy. The geometrical parameter and BO analysis reveal that the TSs are concerted and asynchronous. Moreover, the presence of an EW group on the nitrile oxide results in more asynchronous TSs and the more ER group go through more synchronous TSs. On comparing the reaction of substituted

nitrile oxides with ethene and C_{60}, it can be found that the predicted activation energy and asynchronicity have larger value with C_{60} than with ethene. In spite of the low CT found in these 1,3-DCs, a good correlation between the electrophilicity of the nitrile oxides and the activation energy of the reaction is found; the increase of the electrophilicity of **RCNO** accelerates the reaction towards a C_{60} to nitrile oxide CT process. Finally, the 1,3-DCs of **FCNO**, *via* the less polar TSs, are the fastest reactions. This behavior can be associated with some pseudodiradical character of the cycloaddition, raised by the presence of fluorine substituent. Apart from these, we have the computed structural parameters[40] of the CAs for the reactions of **RCNO** with ethene and C_{60}. We have also predicted the IR spectrum of these CAs.[40] We look forward that these aforementioned data will be helpful to experimentalists in their attempts for the synthesis and characterization of these novel compounds.

ACKNOWLEDGEMENTS

The authors would like to thank anonymous reviewers for their useful comments. Computational facilities offered by Institute of Physical Chemistry of Romanian Academy and from University of Mauritius are acknowledged. This work was supported by funding provided by the Mauritius Tertiary Education Commission (TEC). The authors also gratefully acknowledge discussion with Prof J. M. Dyke from the University of Southampton. This paper is dedicated to Professor A. Padwa: gentleman and uniquely gifted scholar.

REFERENCES

1. H. W. Kroto, J. R. Heath, S. C. O'Brien, R. F. Curl, and R. E. Smalley, *Nature*, 1985, **318**, 162.
2. W. Krätshmet, L. D. Lamb, K. Fostiropoulos, and D. R. Huffman, *Nature*, 1990, **347**, 354.
3. M. A. Yurovskaya and I. V. Trushkov, *Russ. Chem. Bull. Int. Ed.,* 2002, **51**, 367.
4. (a) X. Lu and Z. F. Chen, *Chem. Rev.*, 2005, **105**, 3643; (b) H. Sun, X. Yun, S. Wu, and Q. Teng, *J. Mol. Struct. (THEOCHEM)*, 2008, **868**, 71; (c) Z. F. Chen and R. B. King, *Chem. Rev.*, 2005, **105**, 3613; (d) M. H. O. Rashid, C. Lim, and C. H. Choi, *Bull. Korean Chem. Soc.,* 2010, **31**, 1681.
5. (a) L. B. Piotrovskii, *Ros. Nanotekhnol.*, 2007, **2**, 6; (b) R. Bakry, R. M. Vallant, M. Najam-ul-Haq, M. Rainer, Z. Szabo, C. W Huck, and G. K. Bonn., *Int. J. Nanomed.,* 2007, **2**, 639; (c) Z. Markovic and V. Trajkovic, *Biomaterials,* 2008, **29**, 3561.
6. (a) M. Prato and M. Maggini, *Acc. Chem. Res.,* 1998, **31**, 519; (b) M. Prato, *Top. Curr. Chem.,* 1999, **199**, 173; (c) F. Diederich and M. Gómez-López, *Chem. Soc. Rev.*, 1999, **28**, 263; (d) D. M. Guldi, F. Zerbetto, V. Georgakilas, and M. Prato, *Acc. Chem. Res.,* 2005, **38**, 38.
7. (a) E. Nakamura and H. Isobe, *Acc. Chem. Res.,* 2003, **36**, 807; (b) E. Nakamura and H. Isobe, *Chem. Rec.,* 2010, **10**, 260; (c) R. Maeda-Mamiya, E. Noiri, H. Isobe, W. Nakanishi, K. Okamoto, K. Doi, T.

Sugaya, T. Izumi, T. Homma, and E. Nakamura, *Proc. Natl. Acad. Sci.,* 2010, **107**, 5339.

8. (a) Z. Xiao, F. Wang, S. Huang, L. Gan, J. Zhou, G. Yuan, M. Lu, and J. Pan, *J. Org. Chem.*, 2005, **70**, 2060; (b) N. Martín, M. Altable, S. Filippone, A. Martín-Domenech, M. Güelle, and M. Solà, *Angew. Chem. Int. Ed.,* 2006, **45**, 1439; (c) N. Masakazu, Y. Segawa, and K. Itami, *J. Am. Chem. Soc.,* 2011, **133**, 2402.
9. I. Y. Podolski, Z. A. Podlubnaya, and O. V. Godukhin, *Biophysics,* 2010, **55**, 71.
10. A. Hirsch and M. Brettreich, *Fullerenes: Chemistry and Reactions,* Weinheim, Germany: Wiley-VCH Verlag GmbH & Co. KgaA, 2005.
11. (a) A. Hirsch, *Synthesis*, 1995, 895; (b) W. Silwa, *Fullerene Sci. Technol.,* 1995, **3**, 243; (c) M. A. Yurovskaya, and A. A. Ovcharenko, *Khim. Geterotsikl Soedin.*, 1998, 291 [*Chem. Heterocycl. Compd.*, 1998 (*Engl. Transl.*)]; (d) E. N. Karaulova and E. I. Baggi, *Usp. Khim.,* 1999, **68**, 979 [*Russ. Chem. Rev.,* 1999, **68** (*Engl. Transl.*)].
12. (a) M. Maggini, G. Scorrano, and M. Prato, *J. Am. Chem. Soc.*, 1993, **115**, 9798; (b) M. Prato and M. Maggini, *Acc. Chem. Res.,* 1998, **31**, 519; (c) M. Holzinger, O. Vostrowsky, A. Hirsh, F. Hennrich, M. Kappes, R. Weiss, and F. Jellen, *Angew. Chem.,* 2001, **113**, 4132 [*Angew. Chem. Int. Ed.,* 2001, **40**, 4002]; (d) N. Tagmatarchis and M. Prato, *J. Mater. Chem.*, 2004, **14**, 437; (e) S. Filipponne, M. I. Baraso, A. Martín-Domenech, S. Osuna, M. Solà, and N. Martín, *Chem. Eur. J.*, 2008, **14**, 5198.
13. T. Suzuki, Q. Li, K. C. Khemani, and F. Wudl, *J. Am. Chem. Soc.,* 1992, **114**, 7301.
14. For book, see: (a) A. Hirsch and M. Brettreich, *Fullerenes: Chemistry and Reactions*, Wiley-VCH Verlag GmbH & Co., KGaA, 2005; (b) F. Langa and J.-F. Nierengarten, *Fullerenes: Principles and Applications*, RSC Publishing, 2007.
15. For some recent papers see: (a) F. Liu, W. Du, Q. Liang, Y. Wang, J. Zhang, J. Zhao, and S. Zhu, *Tetrahedron,* 2010, **66**, 5467; (b) H. Kitamura, K. Kokubo, and T. Oshima, *Org. Lett.,* 2007, **9**, 4045; (c) V. A. Ioutsi, A. A. Zadorin, P. A. Khavrel, N. M. Belov, N. S. Ovchinnikova, A. A. Goryunkov, O. N. Kharybin, E. N. Nikolaev, M. A. Yurovskaya, and L. N. Sidorov, *Tetrahedron,* 2010, **66**, 3037; (d) G.-W. Wang, H.-T. Yang, P. Wu, C.-B. Miao, and Y. Xu, *J. Org. Chem.*, 2006, **71**, 4346; (e) G.-W. Wang and H.-T. Yang, *Tetrahedron Lett.*, 2007, **48**, 4635.
16. H.-T. Yang, X.-J. Ruan, C.-B. Miao, and X.-Q. Sun, *Tetrahedron Lett.,* 2010, **51**, 6056.
17. (a) M. S. Meier and M. Poplawska, *J. Org. Chem*., 1993, **58**, 4524; (b) M. S. Meier, D. J. Rice, C. Thomas, V. Majidi, R. Pogue, and M. Poplawska, *Mat. Res. Soc. Symp. Proc.,* 1995, **359**, 369; (c) H. Irngartinger, C. M. Höhler, U. Huber-Patz, and W. Krätshmer, *Chem. Ber.,* 1994, **127**, 581; (d) M. Aulbach, and H. U. Ter Meer (Hoechst AG), DE 4240042, 1994, [*Chem. Abstr.,* 1995, **122**, 31507n]; (e) H. Irngartinger, A. Weber, and T. Escher, *Liebigs Ann.*, 1996, 1845; (f) T. Da Ros, M. Prato, F. Novello, M. Maggini, M. De Amici, and C. De Micheli, *Chem. Commun*., 1997, 59; (g) O. G. Sinyashin, I. P.

Irina, F. R. Sagitova, V. A. Pavlov, V. I. Kovalenko, Y. V. Badeev, N. M. Azancheev, A. V. Ilyasov, A. V. Chernova, and I. Vamdyukova, *Mendeleev Commun.*, 1998, **8**, 43.

18. K. Kavitha and P. Venuvanalingam, *J. Org. Chem*., 2005, **70**, 5426.
19. http://pages.unibas.ch/mdpi/ecsoc/e0002/calelecg.htm.
20. H. Stolzenberg, B. Weinberger, W. P. Fehlhammer, F. G. Pühlhofer, and R. Weiss, *Eur. J. Inorg. Chem.*, 2005, 4263.
21. H. Wang, Y. Wang, K. Han, and X. Peng, *J. Org. Chem.*, 2005, 7**0**, 4910.
22. K. B. Wiberg, *Tetrahedron,* 1968, **24**, 1083.
23. (a) L. R. Domingo, M. T. Picher, P. Arroyo, and J. A. Saez, *J. Org. Chem.,* 2006, **71**, 9319; (b) L. R. Domingo, E. Chamorro, and P. Pérez, *Eur J. Org. Chem.,* 2009, 3036.
24. (a) L. R. Domingo, M. J. Aurell, P. Pérez, and R. Contreras, *Tetrahedron*, 2002, **58**, 4417; (b) P. Pérez, L. R. Domingo, M. J. Aurell, and R. Contreras, *Tetrahedron*, 2003, **59**, 3117; (c) P. Pérez, L. R. Domingo, A. Aizman, and R. Contreras, In *Theoretical Aspects of Chemical Reactivity*: ed. by A. Toro-Labbé; Elsevier Science: Amsterdam, the Netherlands, 2007; Vol. 19, pp. 139-201.
25. P. Jaramillo, L. R. Domingo, E. Chamorro, and P. Pérez, *J. Mol. Struct.: (Theochem*), 2008, **865**, 68.
26. L. R. Domingo and J. A. Saez, *J. Org. Chem.*, 2011, **76**, 373.
27. Gaussian 03, Revision B.03, M. J. Frisch, G. W. Trucks, H. B. Schlegel, G. E. Scuseria, M. A. Robb, J. R. Cheeseman, J. A. Montgomery, Jr., T. Vreven, K. N. Kudin, J. C. Burant, J. M. Millam, S. S. Iyengar, J. Tomasi, V. Barone, B. Mennucci, M. Cossi, G. Scalmani, N. Rega, G. A. Petersson, H. Nakatsuji, M. Hada, M. Ehara, K. Toyota, R. Fukuda, J. Hasegawa, M. Ishida, T. Nakajima, Y. Honda, O. Kitao, H. Nakai, M. Klene, X. Li, J. E. Knox, H. P. Hratchian, J. B. Cross, V. Bakken, C. Adamo, J. Jaramillo, R. Gomperts, R. E. Stratmann, O. Yazyev, A. J. Austin, R. Cammi, C. Pomelli, J. W. Ochterski, P. Y. Ayala, K. Morokuma, G. A. Voth, P. Salvador, J. J. Dannenberg, V. G. Zakrzewski, S. Dapprich, A. D. Daniels, M. C. Strain, O. Farkas, D. K. Malick, A. D. Rabuck, K. Raghavachari, J. B. Foresman, J. V. Ortiz, Q. Cui, A. G. Baboul, S. Clifford, J. Cioslowski, B. B. Stefanov, G. Liu, A. Liashenko, P. Piskorz, I. Komaromi, R. L. Martin, D. J. Fox, T. Keith, M. A. Al-Laham, C. Y. Peng, A. Nanayakkara, M. Challacombe, P. M. W. Gill, B. Johnson, W. Chen, M. W. Wong, C. Gonzalez, and J. A. Pople, Gaussian, Inc., Wallingford CT, 2004.
28. A. D. Becke, *J. Chem. Phys.,* 1988, **38**, 3098.
29. C. Lee, W. Yang, and R. G. Parr, *Phys. Rev. B,* 1988, **37**, 785.
30. W. J. Hehre, L. Radom, P. v. R. Schleyer, and J. A. Pople, *Ab Initio Molecular Orbital Theory;* Wiley: New York, 1986.
31. CYLview, 1.0b; C. Y. Legault, Université de Sherbrooke, 2009 (http://www.cylview.org).
32. (a) C. Gonzalez and H. B. Schlegel, *J. Chem. Phys.,* 1989, **90**, 2154; (b) C. Gonzalez and H. B.

Schlegel, *J. Phys. Chem.,* 1990, **94**, 5523.

33. (a) A. E. Reed, R. B. Weinstock, and F. Weinhold, *J. Chem. Phys.,* 1985, **83**, 735; (b) A. E. Reed, L. A. Curtiss, and F. Weinhold, *Chem. Rev.,* 1988, **88**, 899.
34. R. G. Parr, L. von Szentpaly, and S. Liu, *J. Am. Chem. Soc.,* 1999, **121**, 1922.
35. (a) R. G. Parr and R. G. Pearson, *J. Am. Chem. Soc.* 1983, **105**, 7512; (b) R. G. Parr and W. Yang, *Density Functional Theory of Atoms and Molecules*, Oxford University Press, New York, 1989.
36. W. Kohn and L. Sham, *J. Phys. Rev. A,* 1965, **140**, 1133.
37. L. R. Domingo, E. Chamorro, and P. Pérez, *J. Phys. Chem. A,* 2008, **112**, 4615.
38. (a) D. G. Truhlar, A. D. Issacson, and B. C. Garett, In *Generalized Transition State Theory, Vol 4 of Theory of Chemical Reaction Dynamics,* pp. 65-137, CRC Press, Boca Raton, FL, 1985; (b) M. J. Pilling and P. W. Seakins, In *Reaction Kinetics*, 2nd ed, Oxford Science, Oxford, 1995; (c) P. R. P. Barreto, A. F. A. Vilela, and R. Gargano, *Int. J. Quantum Chem.,* 2005, **103**, 685.
39. E. P. Z. Wigner, *Phys. Chem. B,* 1932, **19**, 203.
40. Supplementary materials are available with the authors upon request.